

A New Control Strategy for Bi-Directional DC-DC Converter in Electric Vehicle

Zhang Xuhui^{1,2}, Xuhui Wen¹, Zhao Feng¹, Guo Xinhua¹

¹Institute of Electrical Engineering Chinese Academy of Sciences, Beijing100190, China

²Graduate University of Chinese Academy of Sciences, Beijing100039, China

Abstract –In order to improve the drive system efficiency, a boost/buck bi-directional DC-DC converter which can regulate the DC-link voltage according to optimal efficiency curve is added between the battery and the traditional voltage source inverters (VSI) supplying a motor. The traditional control approach for the bi-directional DC-DC converter is based on the analog control concept. However, it is not the best choice in digital control environment. In this paper, a new control strategy with a digital control concept is presented which can achieve a smooth switching between the boost and buck operation state using only one controller. The small-signal model of the controller is built and the relationship between the out power and the DC-link voltage stability is discussed. The PMSM drive system in electric vehicles (EV) is modeled using MATLAB/simulink and a operation condition in EV is simulated to verify the above theoretical analysis. The simulation and theoretical analysis results match with good agreement.

I. INTRODUCTION

The DC side of traditional VSI in EV is connected directly in parallel with battery and capacitors. Due to the battery voltage is not adjustable, it will cause a low efficiency of the drive system because the main losses in drive system including motor losses, inverter losses, and converter losses are all related with the DC-link voltage. To overcome the above shortcoming, a boost/buck bi-directional DC-DC converter as shown in the dotted green block in Fig.1 is added to the drive system. The main role of DC/DC converter is to regulate the DC-link voltage according to the adjustable optimal efficiency curve of the drive system.

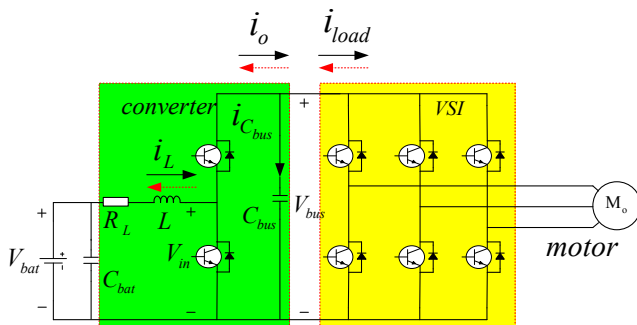


Fig.1 Configuration and power flow of the converter–inverter system.

Because the motor operates in four-quadrant, the bi-directional DC/DC converter should switch its operation state according to that of motor. If using a traditional control approach [1], it needs a boost and a buck controllers and a switching logic for them to guarantee the DC-link power balance. To simplify the above controllers, an integrated controller is presented that switches the both IGBTs using two complementary non-overlapped PWM signals and thus it achieves a smooth bi-directional switching [2]. The above control approaches are all based on the analog controls idea

and all use PI controllers to compensate the transfer function from duty cycle to inductor current or bus voltage. Its disadvantage is difficult to optimize the control strategy more deeply.

In this paper, the converter–inverter system in Fig.1 is controlled as a special back-back system [3]. Hence the difference between novel control methods and the traditional one is the battery voltage feed forward in the inner current control loop that cause the transfer function of the inner current control loop only relevant to the inductor parameters and the PI parameters. Therefore, it can keep a large range system stability using only one set of PI parameters.

The paper is organized as follows. Firstly, the control strategy for the bi-directional DC-DC converter is proposed according to its state equations. Secondly, the output current impact on the bus voltage is analysis based on the small-signal mode of the controller. Then, under the different power flow direction of the constant power load, several factors that affect the system stability are analyzed. Finally, the simulation model of drive system including the DC/DC converter is built. A test operation condition of EV is simulated and the simulation results confirm the correctness of the above theoretical analysis.

II. The New Control Strategy for Bi-Directional DC-DC Converter

In this paper, the positive reference direction of currents is determined with the black solid arrow in Fig.1. If the motor operates under motor-driven state, the energy flows from the battery to the DC-link while the converter acts as a boost converter. Otherwise, the energy flows from DC-link to the battery if the motor operates under regenerative braking state while the converter acts as a buck converter. Here the complementary control logic of the two IGBTs is used, so the inductor current is always in continuous current mode (CCM). By choosing the DC-link voltage V_{dc} and inductor current i_L as the states, the variable relationship of bi-directional DC-DC converter using state space averaged method is described as [4]:

$$L \frac{di_L}{dt} + i_L R_L = V_{bat} - V_{in} \quad (1)$$

$$C_{bus} \frac{dV_{bus}}{dt} = i_o - i_{load} \quad (2)$$

$$V_{bat} i_L = V_{bus} i_o \quad (3)$$

where V_{bat} denotes battery voltage, V_{in} denote a new voltage variable, i_o denotes the current from the DC/DC converter to the DC-link and the i_{load} denotes the current from DC-link to the inverter and i_{Cbus} , L and C_{bus} denotes inductance of the

inductor and DC-link capacitance, respectively, R_L denotes equivalent series resistance of inductor.

Fig.2 shows the block diagrams of the PI dual-loop controller for the converter according to equations (1)-(3).

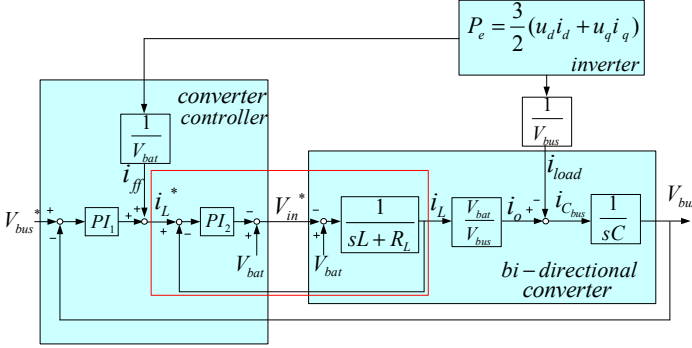


Fig.2 Block diagram of the proposed controller of bi-directional converter

Due to the DC-link voltage V_{bus} variation caused by the change of the current, the direct approach to minimize DC-link capacitor is attempting to make no current flows into C_{bus} . For this reason, the inverter output power information is used in the control scheme to make the converter control action fast, and then make the converter side current i_o the same as the inverter side current i_{load} at the DC-link. So let:

$$P_e = 3/2(u_d i_d + u_q i_q) \quad (4)$$

where P_e denotes the output electromagnetic power of the motor, u_d and u_q denotes the d - q axes motor stator voltage, and i_d and i_q denotes d - q axes motor stator current in a synchronous reference frame.

So if the motor operates under motor-driven state, P_e is positive and generates a positive inductor reference current. On the other hand, if the motor operates under braking state, P_e is negative and generates a negative inductor reference current.

The closed loop transfer function of the current i_L can be derived as:

$$\frac{i_L}{i_L^*} = \frac{K_{p2}s + K_{i2}}{Ls^2 + (K_{p2} + R_L)s + K_{i2}} \quad (5)$$

where K_{p2} , K_{i2} are the proportional and integral parameters of inner current control loop.

The zero and one of the poles in (7) are designed to cancel with each other by letting:

$$K_{i2} / K_{p2} = R_L / L \quad (6)$$

which results in:

$$\frac{i_L}{i_L^*} = \frac{K_{p2} / L}{(s + K_{p2} / L)} = \frac{1}{Ts + 1} \quad (7)$$

where $T=L/K_{p2}$

The bandwidth of the current loop is therefore K_{p2}/L . In this study, the current loop bandwidth is set at 2kHz considering the switching frequency is 10kHz. The $L=0.2\text{mH}$, $R_L=0.01\text{ohm}$ and the parameters of the PI controller are calculated to be $K_{p2}=0.4$, $K_{i2}=20$.

In the converter controller i_L is utilized to regulate V_{bus} , while i_{load} is treated as a disturbance. To analyze the

disturbance suppression of controller, the small-signal relation between the DC-link variables and the battery variables may be obtained by first order Taylor series expansion of (2) and (4).

$$sC\tilde{v}_{bus} = \tilde{i}_o - \tilde{i}_{load} \quad (8)$$

$$\tilde{i}_o = \frac{V_{bat}}{V_{bus}} \tilde{i}_L - \frac{I_o}{V_{bus}} \tilde{v}_{bus} \quad (9)$$

where \tilde{i}_o , \tilde{v}_{bat} , \tilde{i}_L , \tilde{v}_{bus} is disturbance value of output current, battery voltage, load current and DC-link voltage respectively.

According to the feed-forward current term in Fig.2, the feed-forward current is:

$$I_{ff} = \frac{V_{bus}}{V_{bat}} I_{load} \quad (10)$$

where I_{ff} is steady-state value of feed-forward current term. Then the small-signal expression of (12) is obtained:

$$\tilde{i}_{ff} = \frac{V_{bus}}{V_{bat}} \tilde{i}_{load} \quad (11)$$

where \tilde{i}_{ff} , \tilde{i}_{load} is disturbance value of I_{ff} and I_{load} respectively.

By using the small-signal expressions of equations (10)-(11), the diagram of the small-signal model of the converter controller is shown in Fig.3.

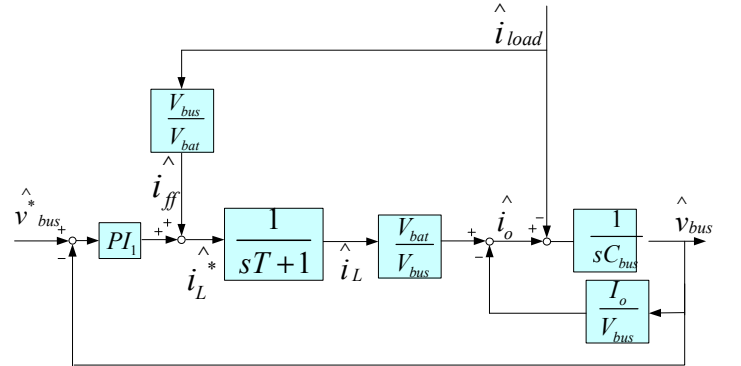


Fig.3 Small-signal model of the bi-directional converter controller

Based on the small-signal model of the boost converter controller, it is easily to derive the transfer functions from the output current to DC-link voltage as:

$$\frac{\tilde{v}_{bus}}{\tilde{i}_{load}} = \frac{-Ts^2}{TC_{bus}s^3 + (C_{bus} + \frac{TI_o}{V_{bus}})s^2 + (\frac{K_{p1}V_{bat}}{V_{bus}} + \frac{I_o}{V_{bus}})s + \frac{k_{i1}V_{bat}}{V_{bus}}} \quad (12)$$

where K_{p1} and K_{i1} are the proportional and integral parameters of the outer voltage control loop.

It can be seen in (12) that the feed-forward term can almost eliminate the effect from output current disturbance to DC-link voltage if the T is small enough. Fig. 4 shows the Bode plots of (12) when the converter operates as a boost converter while $V_{bat}=200\text{V}$, $V_{bus}=400\text{V}$, $I_o=50\text{A}$, $K_p=5$, $K_i=0.1$, $T=0.5\text{ms}$ or 0.4ms and $C_{bus}=550\mu\text{F}$ or $1000\mu\text{F}$. It is clear that a large DC-link capacitor is also beneficial to suppress the voltage disturbance caused by output current.

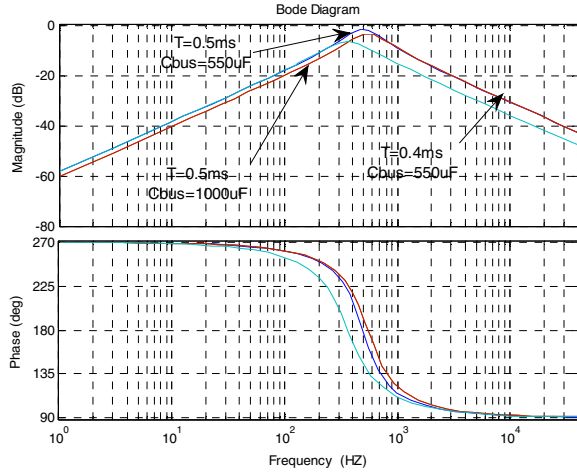


Fig. 4 Bode plots of the transfer function from i_{load} to v_{bus}

III. SMALL-SIGNAL STABILITY ANALYSIS OF THE PROPOSED CONTROLLER

When the speed and torque of motor under motor-driven state are regulated in Fig.1, the inverter will appear as a “constant power” load to the DC bus and have a negative incremental input admittance as shown in right-half plane of Fig.5. Therefore, the inverter acts as loads of the boost converter and the special load may easily cause the DC bus voltage instability than the common resistive load [5]. However, when the motor operates under generating state, a “constant power” flows into the DC-link and DC-link voltage stability problem in this case has not been studied so far.

In this section, the DC-link voltage stability of the converter loaded by a constant power load is studied. By using the state-space averaging method, the state-space equations of converter in Fig.1 are changed as:

$$C_{bus} \frac{dV_{bus}}{dt} = \frac{V_{in} I_L}{V_{bus}} - \frac{P_e}{V_{bus}} \quad (13)$$

$$L \frac{di_L}{dt} + R_L i_L = V_{bat} - V_{in} \quad (14)$$

The small-signal expressions of equations (13)-(14) are described as (15) and (16):

$$\tilde{v}_{bus} = \frac{I_L (sL + R_L) - V_{bat}}{sC(sL + R_L)V_{bus}} \tilde{v}_{in} - \frac{\tilde{P}_e}{sCV_{bus}} \quad (15)$$

$$\tilde{i}_L = -\tilde{v}_{in} / (sL + R_L) \quad (16)$$

where \tilde{v}_{in} , \tilde{P}_e is the disturbance of V_{in} and P_e respectively.

By using the small-signal expressions (15) and (16), the diagram of the small-signal model including the dual control loops of the converter controller is shown in Fig.6.

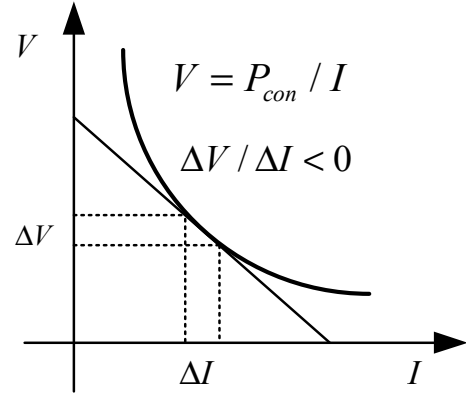


Fig.5 The negative impedance of CPL

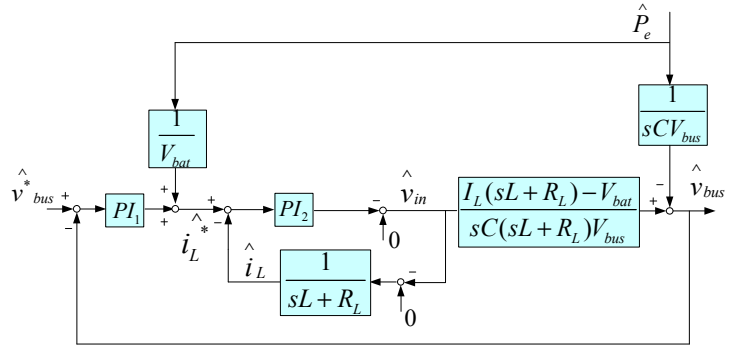


Fig.6. Small-signal model of bi-directional converter with the proposed controller

Since the analysis is focused on the effect on the DC-link voltage variation caused by the load power, the transfer function from \tilde{P}_e to \tilde{v}_{dc} is derived as:

$$\frac{\tilde{v}_{dc}}{\tilde{P}_e} = \frac{-\{[I_L(sL + R_L) - V_{bat}]G_{PI2} / V_{bat} + (sL + R_L)[1 + G_{PI2} / (sL + R_L)]\}}{sC_{bus}(sL + R_L)V_{bus}[1 + G_{PI2} / (sL + R_L)] - \{[I_L(sL + R_L) - V_{bat}] - V_{bat}\}G_{PI1}G_{PI2}} \quad (17)$$

where $G_{PI1} = K_{P1} + K_{i1}/s$, $G_{PI2} = K_{P2} + K_{i2}/s$.

For comparison purpose, Fig.7 shows the poles location of the transfer function from \tilde{P}_e to \tilde{v}_{bus} based on (17) with different parameters when the motor operates in drive state. Here the factors that affect the system stability in (18) is analyzed by changing C_{bus} from 550 μ F to 600 μ F or V_{bus} from 400V to 500V while $L = 0.2$ mH, $V_{bat} = 200$ V, $I_L = 100$ A, $K_{PI1} = 9.5$, $K_{i1} = 10$, $K_{PI2} = 0.4$, $K_{i2} = 20$.

It can be seen in Fig.7 that one pair of poles of (19) is in the right-half plane and indicates an instability with a smaller DC-link capacitor. However, with the increase of DC-link voltage or DC-link capacitor, this pair of poles moves into the left-half plane and the system becomes stability. So it is proved that the larger DC-link capacitance or the higher DC-link voltage all benefit the system stability.

Fig.8 shows the DC-link voltage instability difference between the positive power and negative power flow into the DC-link while the other parameters are same as in (18). It can be seen that the positive power cause an instability DC-link voltage which corresponding to the motor operate under motor-driven state. However, the same power flow into the DC-link when the motor operates under regenerative braking state, the

DC-link voltage is still stable. Therefore, the stability problem under the motor-driven state in this drive system should be solved in more important position.

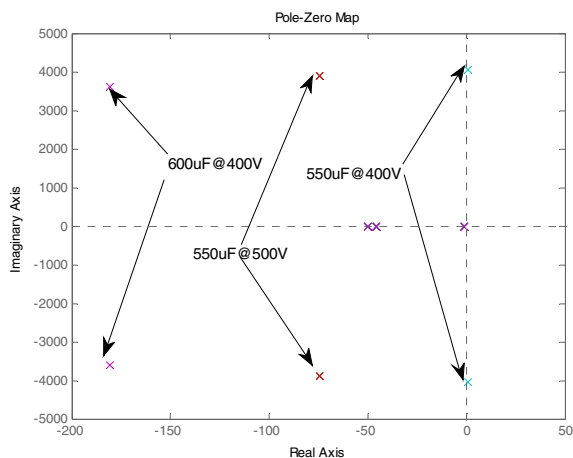


Fig.7 Poles distribution of the transfer function from p_{mv} to v_{bus} with different parameters

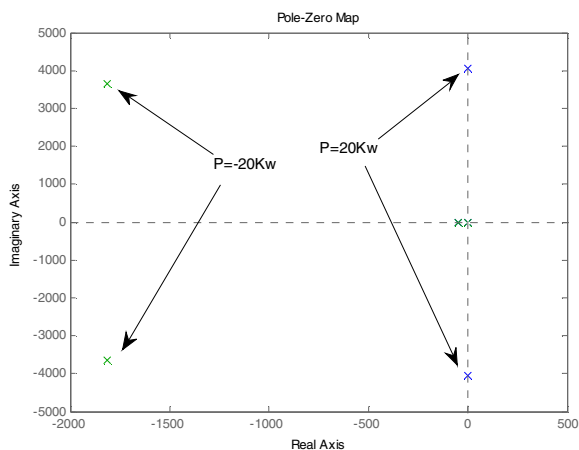


Fig. 8 Poles distribution of the transfer function from p_{mv} to v_{bus} under different power flow direction

IV. SYSTEM SIMULATION RESULTS AND DISCUSSION

In order to verify the above theoretical analysis, the drive system simulation model in Fig.1 is built using MATLAB/simulink which includes PMSM drive system and the DC/DC converter controller.

Fig.9 shows the simulation results using the drive system simulation model. The red line is the simulation curve with a larger 600uF DC-link capacitor and the blue one is with a smaller 520uF DC-link capacitor. It can be seen that a higher C_{bus} capacitance is beneficial to the DC-link voltage stability. However, the DC-link voltage does not fluctuate even with a smaller capacitor when the DC-link voltage is adjusted from 400V to 500V. In addition, a motor power flows into the DC-link under the regenerative braking state is beneficial to stabilize the DC-link voltage than that flows out the DC-link when the motor operates under motor-driven state. So, all the simulation results verify the theoretical analysis in the above section.

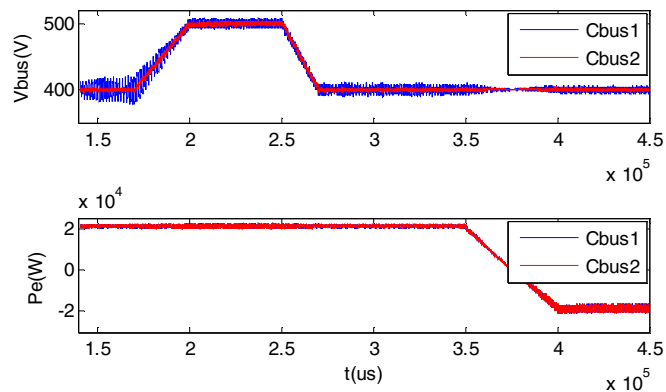


Fig.9. Simulation results of the relationship between DC-link voltage and output power

V. CONCLUSION

In this paper, the new drive system with the boost/buck bi-directional DC-DC converter is controlled as a special back-back system. The small-signal model of it shows that a fast inner current control loop and a large DC-link capacitor are beneficial to suppress the DC-link voltage disturbance more effectively. In addition, the motor-driven mode is more likely to cause the DC-link voltage instability than the regenerative braking state. And the drive system simulation model proves the above theoretical analysis by using running under a typical operation condition.

ACKNOWLEDGMENT

This work was supported by the National Natural Science Foundation of China under Project 61034007.

VI. REFERENCES

- [1] Haiping Xu, Xuhui Wen, Li Kong, "DSP-based digitally controlled bi-directional DC-DC converter" Industrial Electronics Society, 2004. IECON 2004. 30th Annual Conference of IEEE .
- [2] Zhiling Liao, Xinbo Ruan, "Control strategy of bi-directional DC/DC converter for a novel stand-alone photovoltaic power system" Vehicle Power and Propulsion Conference, 2008. VPPC '08. IEEE
- [3] Gu B G, Nam K.A Dc-link capacitor minimization method through direct capacitor current control. IEEE Transactions on Industry Applications. 2006, 42 (2):573-581.
- [4] J. Sun, D. M. Mitchell, M. F. Greuel, P. T. Krein and R. M. Bass, Averaged modeling of PWM converters operating in discontinuous conduction mode, IEEE Transactions on Power Electronics, 16(4), 2001, 482-492.
- [5] A. Emadi, and M. Ehsani, "Negative Impedance Stabilizing Controls for PWM DC/DC Converters Using Feedback Linearization Techniques," IEEE Intersociety Energy Conversion Engineering Conference, 2000, Vol.1, pp.613-620.